Journal of Solid State Chemistry **147,** 199–210 (1999)
Article ID jssc.1999.8213, available online at http://www.idealibrary.com on IDEAL®

Electrochemical and Chemical Behavior of Extra Molybdenum Atoms into the Chevrel Phase Host Network

Z. Kaidi,* S. Belin,† C. Boulanger,* J.-M. Lecuire,* M. Sergent,† and R. Chevrel†,[1]

*Laboratoire d'Electrochimie des Matériaux, UMR CNRS 7555, Université de Metz, Ile du Saulcy, 57045 Metz Cedex 01, France; and
†Laboratoire de Chimie du Solide et Inorganique Moléculaire, UMR CNRS 6511, Campus de Beaulieu, Université de Rennes 1, 35042 Rennes Cedex, France
E-mail: chevrel@univ-rennes1.fr

Received November 25, 1998; accepted February 5, 1999

In this paper, we present a comparative electrochemical study of copper insertion into series of $Mo_6Se_{8-x}S_x$ phases which are obtained through different synthesis processes. We show that α-, β-, and HT-forms can reversibly accommodate copper at room temperature. The variation of the integral copper insertion rate is a function of the sulfur content and the synthesis type of pseudobinaries. While the mechanism of copper intercalation is quite similar for the different $Mo_6Se_{8-x}S_x$ for a given x, there is a drastic difference for α- and β-Mo_6S_8 compound. This behavior is explained on the basis of structural considerations. If the extra Mo atoms, present in the lattice channels of the β form and HT-$Mo_6Se_{8-x}S_x$, are not displaced by this copper intercalation, they are shown to be mobile through cationic exchange reactions and chemical deinsertion at higher temperature. © 1999 Academic Press

Key Words: **Chevrel phases; copper; electrochemistry; intercalation; cationic exchange.**

I. INTRODUCTION

The Chevrel phases $M_xMo_6X_8$ (M = metal ion; X = S, Se, Te) present interesting physical properties (superconductivity and high critical magnetic fields, coexistence of superconductivity and magnetism) (1, 2). These properties have been found to strongly depend upon the nature of chalcogen X, cation M, and its content x. These compounds are characterized by a framework matrix built-up from quasi-rigid Mo_6X_8 molecular units. The three-dimensional packing of these Mo_6X_8 units leads to a system of channels along the rhombohedral axes which can accommodate the ternary metal atoms (M).

In addition to these physical properties, these phases exhibit a remarkable chemical reactivity. The high mobility of the guest atom in the open framework type structure allows to the synthesis of a series of new metastable compounds by means of low-temperature chemical or electrochemical topotactic redox reactions via electron/ion transfer process (3–8):

$$M_xMo_6X_8 - xne^- \Leftrightarrow Mo_6X_8 + xM^{n+}.$$

This type of solid state reaction provides a way to obtain the α-$Mo_6Se_{8-x}S_x$ mixed binaries series for instance by oxidation of ternary phase in an aqueous hydrochloric acid solution (3). These binaries are then transformed into a new series of phases by annealing, which are called β. It can be noted that the usual high temperature ceramic synthesis only gives $Mo_6Se_{8-x}S_x$ binaries for $x \leq 5$ so-called HT phases. Recently, it has been shown that these β-$Mo_6Se_{8-x}S_x$ and HT-$Mo_6Se_{8-x}S_x$ binaries correspond to pseudo-ternaries with Mo guest atoms located in the channels of the host network (9–11).

Two main ideas emerged to study the mobility of these molybdenum atoms (Mo(2)) in the host. First, we searched some process to remove these extra Mo(2) atoms from the channels. Second, we studied the accommodation capacity of the new host network with extra Mo(2) atoms through the overinsertion of cations. The Chevrel phases can be characterized by the valency electron concentration (VEC), i.e., the number of valence electrons on the metal–metal bondings of the Mo_6 cluster, which takes into account the number of valence electron that a metal ion can transfer to the Mo cluster. The host network Mo_6S_8 has a VEC = 20e/Mo_6, and Mo_6Se_8 has a VEC = 21e/Mo_6 (12). The host Mo_6X_8 network can theoretically accommodate metal ions until a VEC value as high as 24e/Mo_6. The recently reported β- and HT-$Mo_6Se_{8-x}S_x$ series (9–11) were found to have a VEC inferior or equal to 22e/Mo_6, so we can expect to overinsert some cations in such compounds as it was already shown in other ternary Chevrel phases (13).

Two "soft" routes are here investigated. An important electrochemical study is carried on these materials since electrochemistry is most appropriate to investigate the accommodation capacity of a host network. Soft chemistry

[1] To whom correspondence should be addressed.

0022-4596/99 $30.00

studies (cationic exchange solid state reaction and chemical deintercalation process) are also used to characterize the mobility of the Mo(2) guest atoms.

We report in this context the results of our investigations. It was of interest, therefore, to perform an electrochemical study on topotactic properties of these different binary and pseudo-ternary systems in order to compare their reactivity. Since the copper systems were the subject of a large amount of theoretical and experimental works because the possible use of Mo_6X_8 and $Cu_2Mo_6X_8$ as cathode material in room temperature secondary lithium batteries (14–18), we have chosen to study more specifically this Cu cation intercalation. Finally, a new chemical Mo deintercalation process is reported.

II. EXPERIMENTAL

The topotactic reaction is experimentally followed using the curve $i = f(E)$ with a classical three-electrode device in a thermostated cell (60°C) and under an inert atmosphere (argon HP).

II.1. Electrodes and Electrolytes

Crystallite bed electrodes are prepared according to the already described procedure (7). The powdery samples are applied to the surface of a glassy carbon rod (Société Le Carbone Lorraine) by means of a colloidal graphite slurry (Societé Siceron KF). The electrode so realized was kept immobile in the regularly stirred solution. All potentials are controlled and expressed by reference to the aqueous KCl saturated calomel electrode (SCE). The counter electrode was a platinum wire.

The electrolytes were prepared from copper sulfate (analytical grade Prolabo).

A computer-driven Radiometer IMT1 electrochemical interface and a PJT 24-1 potentiostat/galvanostat were used for cyclic voltametric analysis.

II.2. Samples

Different process are used to synthesize α-Mo_6X_8, β-Mo_6X_8, and HT-Mo_6X_8 compounds. The former ones are obtained by the reaction of stoichiometric mixtures of elemental Ni and Mo, and binary $MoSe_2$ and/or MoS_2 powders into sealed evacuated silica tubes brought to 1200°C over 1 week. This leads to the formation of $Ni_yMo_6X_8$ ternaries, which after hydrochloric acid leaching, yield the α-Mo_6X_8 phases.

β-Mo_6X_8 compounds result from annealing under vacuum of the α-series at appropriated temperatures during 1 or 2 days (9, 10).

The process used to obtain the HT-Mo_6X_8 compounds is the same as that described for the $Ni_yMo_6X_8$ ternary compounds, that is, a ceramic route from the starting elements or binaries (11).

II.3. Controls

X-ray diffraction data are obtained on an Inel C.P. 120 diffractometer with a curved localization detector.

The stoichiometry was determined with an electron microprobe microanalyzer (Cameca SX 50) after embedding and polishing the microcrystals. The elements Cu, Mo, S, and Se were analyzed in twelve different microcrystals of all the samples. The stoichiometry corresponds to the average of these 12 values and is calculated with a number of chalcogen (S + Se) per compound assigned and equal to 8 and with a confidence rate to 95%.

III. ELECTROCHEMICAL DEINSERTION BEHAVIOR OF β-Mo_6S_8

Taking into account the action of anhydrous HCl gas (9), the β-Mo_6S_8 samples were electrochemically oxidized in 1 M aqueous Na_2SO_4 at ambient temperature. Figure 1 shows the anodic scans. Attempts to remove the Mo(2) located in the cavities (1) of the channels by an oxidation at +700 mV have been unsuccessful. This anodic treatment does not induce a change in the Mo composition of the solid. The comparison between the voltamperograms obtained with this pseudo-ternary and those corresponding to the α-binary proves a similarity which can be attributed to the destruction of the host lattice. Similar behavior in aqueous medium and at room temperature were observed in the case of phases with large cations such as Pb^{2+}, Ag^+ located in the same cavity (1). The difficulty to separate the characteristic signal of electrochemical deinsertion and that of the host lattice oxidation is in a relation with channel size. Moreover, the structure of β-Mo_6S_8 reveals that pairs of Mo atoms bonded together are present in the cavity (1). These $(Mo)_2^{4+}$ species may be not very mobile inside the framework at room temperature.

IV. ELECTROCHEMICAL INSERTION OF CADMIUM INTO β-Mo_6S_8

We tried to obtain the α-Mo_6S_8 metastable binary from the β-Mo_6S_8 pseudo-ternary by a Mo electrochemical displacement. We had shown, in early work, that the $In_2Mo_{15}Se_{19}$ phase can be converted to $Mo_{15}Se_{19}$ by an overintercalation of cadmium. The $In_2Mo_{15}Se_{19}$ phase is not the only one for which the ternary element (M) can be electrochemically displaced. Tarascon *et al.* have studied the displacement of M = Ag (19), In, or Tl (5) by lithium in MMo_6S_8. A similar type of reaction occurs with small cations (17, 20).

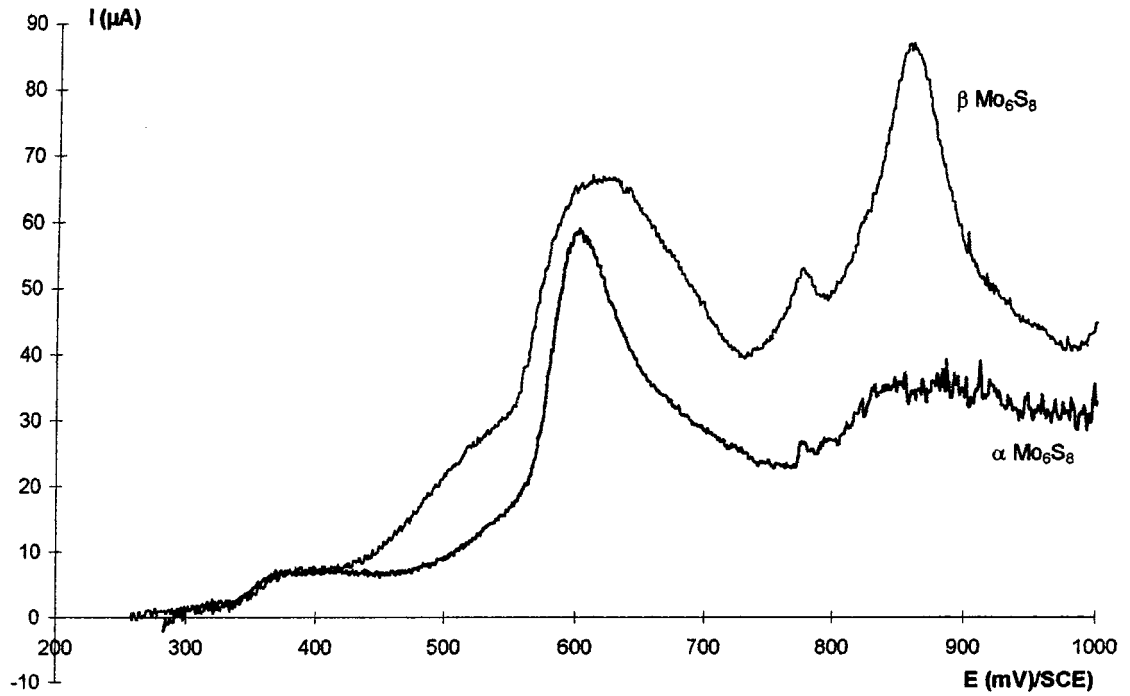

FIG. 1. Voltamperogram for β-Mo_6S_8 compounds in 1 M Na_2SO_4 medium, supporting disk area, $s = 6.2\,mm^2$, temperature $T = 60°C$, scan rate $v = 10\,mV\,min^{-1}$.

The curves of the electrochemical insertion of cadmium are shown in Fig. 2. Several features can be observed. The first potentiodynamic cycle exhibits only one signal ($E^\circ = -550\,mV$) which is small as compared to the corresponding Cd^{2+} intercalation peak in α-Mo_6S_8. Additional voltametric scans reveal a transformation of the voltamperograms. An extra peak located at $-450\,mV$ shows up. This peak slightly grows on subsequent cycles while the first

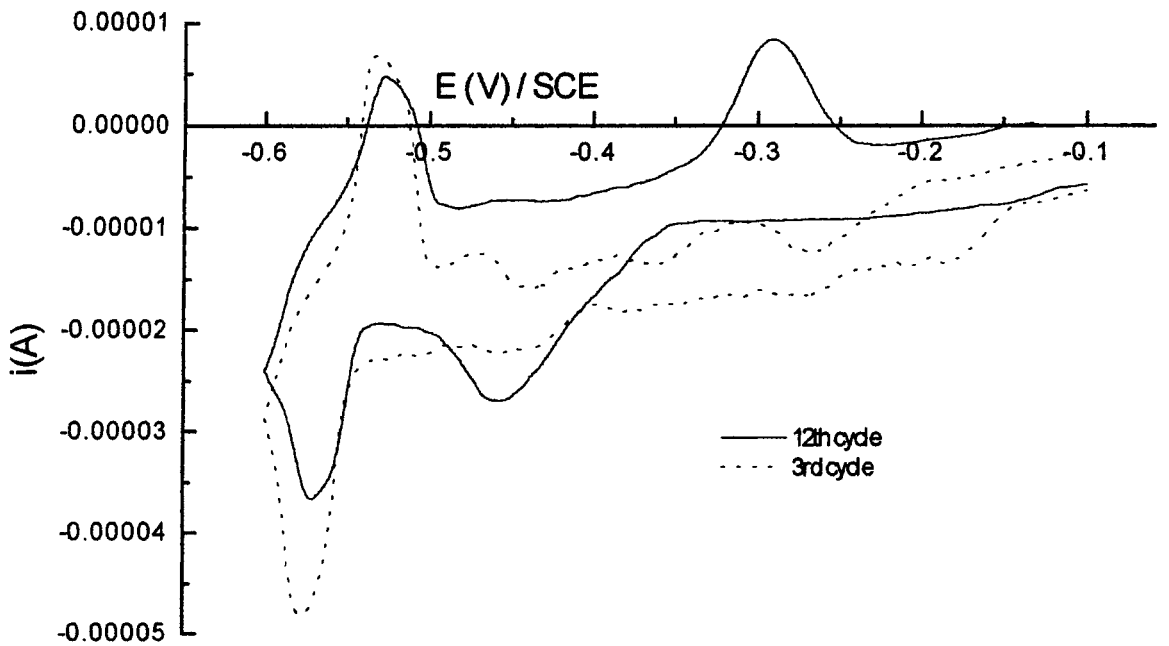

FIG. 2. Voltamperogram for β-Mo_6S_8 in 1 M $CdSO_4$ medium, supporting disk area, $s = 6.2\,mm^2$, temperature $T = 60°C$, scan rate $v = 10\,mV\,min^{-1}$.

one decreases. The voltamperogram features remain constant after 10 cycles. However, one should mention that the electrochemical signals have very low intensities. This observation suggests that only the surface sites are concerned by the intercalation of cadmium and that the cation does not progress through the channels. The migration of Cd^{2+} into the sites would be blocked by $(Mo–Mo)_2^{4+}$ species. The available sites in $MoMo_6S_8$ are certainly not large enough to accommodate large ions such as Cd^{2+}. X-ray diffraction measurements evidenced the absence of structural changes within the β-Mo_6S_8.

The present results clearly indicate that no extra molybdenum (2) atoms can be removed from the host lattice by an electrochemical treatment (oxidation or displacement by cadmium). The low mobility of Mo atoms into the latter phase is uncompatible with a work at ambient temperature.

We then extended the study to the copper intercalation for phases of α- and β-$Mo_6Se_{8-x}S_x$ systems. The family of these different compounds could constitute an ideal example to illustrate the relationship between structure and electrochemistry.

V. ELECTROCHEMICAL INSERTION OF COPPER INTO $Mo_6Se_{8-x}S_x$

V.1. α-$Mo_6Se_{8-x}S_x$

Mo_6S_8, $x = 8$. The electrochemical copper insertion curve (Fig 3a) shows several signals. The voltamperogram feature depends on the potential sweep rate. A slow sweep rate (10 mV min^{-1}) allows successive steps of the insertion to be precisely distinguished. The curve exhibits one first signal which corresponds to a superposition of two signals (an important one $E'_c = 330$ mV and a small one $E''_c = 300$ mV) followed by two other perfectly defined ($E'''_c = 190$ mV, $E''''_c = 140$ mV).

Our study has shown that the stoichiometries of the successive phases are $Cu_{1.27}Mo_6S_8$, $Cu_{1.45}Mo_6S_8$, $Cu_{2.60}Mo_6S_8$, and $Cu_{3.50}Mo_6S_8$. We can bring these insertion rates closer to those obtained by Schöllhorn in an intensiostatic process (14). The phase limits given by this author are $Cu_{1.2}Mo_6S_8$, $Cu_2Mo_6S_8$, and $Cu_{3.2}Mo_6S_8$. Several definite changes were also reported for $0.7 < Cu < 1.2$. The number of steps is homogeneous in the two electrochemical process if the small and poorly differentiated signal is attributed to the mentioned changes. As is expected, the cation rates in the intensiostatic insertion are slightly inferior to those obtained in potentiostatic process.

Another feature arises from the examination of the signals position. In a previous study, we reported that the exploitation of voltamperograms allows the calculation of ΔG free energy of formation of the ternary phases according to $yCu^{\circ} + Mo_6S_8 \rightarrow Cu_yMo_6S_8$ (21). On the basis of equation, the electrochemical insertion in the first potential range ($350 < E < 250$ mV) gives rise to higher stability phases than those obtained in the range ($250 < E < 0$ mV). This result may be explained in terms of site energy which determine the occupancy of these sites by copper. Dudley *et al.* have shown that the large cavities (site 1) are the lowest energy sites which begin to be populated.

The experimental curve suggests the successive occupancy of two types of available sites. The first signals between 350 and 250 mV correspond to the occupancy of the sites 1 while the second potential range indicates lower free energy reactions thus the filling of site 2. To substantiate these suggestions, X-ray diffraction measurements were performed. We have found (Table 1) that the lattice constants of the ternary compounds obtained in the first potential range agree with phases having a copper content inferior to 1.5 while the second one leads to the formation of richer copper compounds. Moreover, it can be noted that there is a broad correspondence between the energy level model proposed by Dudley and the crystallographic data given by Yvon (22). Our results are in good agreement with the results of structural investigations confirming the above suggestions.

We now present the electrochemical and structural results for the α-$Mo_6Se_{8-x}S_x$ ($x = 7, 6, 4, 2, 1, 0$). The electrochemical behavior is reported in Figs. 3b–g, the X-ray results are shown on Table 1. The given stoichiometry (Table 1) for each binary is obtained for the final step, just before the formation of metallic copper by imposing a constant potential to the cathodes during 2 h.

$Mo_6Se_1S_7$, $x = 7$. The general shape of the $i = f(E)$ curve (Fig. 3b) is similar to that exhibited by a α-Mo_6S_8 electrode although the signals are not so well defined. Four intercalation signals can be observed. The cathodic peak potentials are slightly shifted in the potential scale ($E_c = 300$, 225, 160, and 100 mV), but only two global oxidation peaks are distinguished at anodic sweep even if we can suppose the existence of supplementary steps which could certainly be seen by using a slower scan in potential. A copper content of 2.65 for the limit phase is determined leading logically to an increase of cell volume.

$Mo_6Se_2S_6$, $x = 6$. The trend initiated, in the previous case, by the substitution with selenium in the Mo_6S_8 unit is confirmed for this binary, namely poorly differentiated insertion signals (Fig. 3c) and two main oxidation areas (the first one centered at 250 mV and the second one at +350 mV). The shift to a more cathodic intercalation potential becomes more pronounced. The stoichiometry of limit phase is reaching a final value of 2.52 Cu by $Mo_6Se_2S_6$ unit. The cell parameters (Table 1) reveal the presence of cations in channels.

$Mo_6Se_4S_4$, $x = 4$. From this selenium content, the voltamperograms are less complex (Fig. 3d). The insertion arises in two successive steps. The first one takes place from

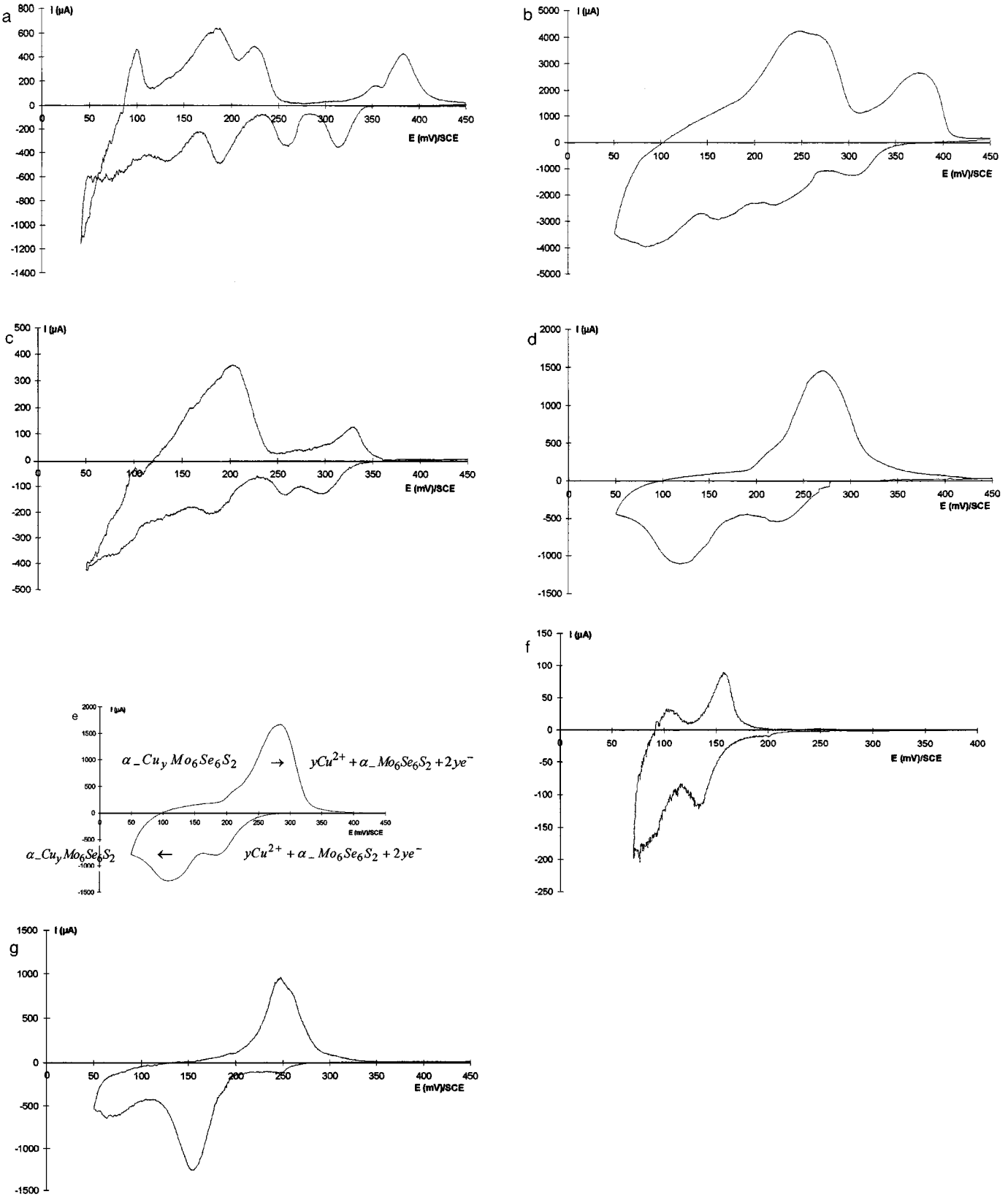

FIG. 3. Voltamperograms for α-$Mo_6Se_{8-x}S_x$ compounds in 1 M $CuSO_4$ medium, supporting disk area, $s = 6.2\,mm^2$, temperature $T = 60°C$, scan rate $v = 10\,mV\,min^{-1}$; (a) $x = 8$, (b) $x = 7$, (c) $x = 6$, (d) $x = 4$, (e) $x = 2$, (f) $x = 1$, (g) $x = 0$.

TABLE 1
Hexagonal Lattice Parameters, Unit Cell Volumes, Analytical Data of α-$Mo_6Se_{8-x}S_x$ Binaries and α-$Cu_yMo_6Se_{8-x}S_x$ Ternaries Prepared by Cathodic Reduction in Copper Aqueous Electrolyte

Phase	Parameters of initial binary			Parameters of intercalated compund			Cu content determined by microprobe analysis	Observations and Cu conent estimation from literature data
	a_h (Å)	c_h (Å)	V_h (Å^3)	a_h (Å)	c_h (Å)	V_h (Å^3)		
					250 mV			
α-Mo_6S_8	9.20	10.88	797	9.40	11.32	809	1.13	1 (1)
					100 mV			
				9.69	10.22	831	3.72	2.7 (1)
α-$Mo_6Se_2S_6$	9.33	10.82	816	9.79	10.35	860	2.52	Intercalation
α-$Mo_6Se_4S_4$	9.42	10.90	837	9.72	10.47	855	1.67	< 2 (24)
α-$Mo_6Se_6S_2$	9.48	11.03	859	9.94	10.60	907	2.26	2.6 (23)
α-$Mo_6Se_7S_1$	9.53	11.10	873	9.96	10.63	914	2.12	Intercalation
α-Mo_6Se_8	9.54	11.21	884	9.97	10.75	926	2.14	2 (12)

280 to 200 mV while the second step is centered at 125 mV. The anodic scan gives evidence for only one wide signal with a little shoulder. A kinetic phenomenon is probably responsible for this electrochemical behavior. The insertion rate (Table 1) stabilizes at a value of 1.67.

$Mo_6Se_6S_2$, $x = 2$. The potentiodynamic curve (Fig. 3e) presents an obvious similarity with that corresponding to the precedent binary, both in shape and in number of signals, though it does not agree in potential scale. The intercalation systems (either in reduction or in oxidation) occur at rather lower values of potential and arises the formation of $Cu_{2.26}Mo_6Se_6S_2$. The crystallographic study gives clear evidence of a structural modification (Table 1). The hexagonal lattice constants observed for this limit phase agree with literature data ($Cu_{2.6}Mo_6Se_{6.5}S_{1.5}$ described by Mc Kinnon (23)).

$Mo_6Se_7S_1$, $x = 1$. The same general observations (Fig. 3f) can be noted for this value of x. The copper content for the $Mo_6Se_7S_1$ is equal to 2.12 for an intercalated phase obtained at 100 mV.

Mo_6Se_8, $x = 0$. The voltamperogram (Fig 3g) exhibits a significant signal ($E = 150$ mV). Additional potential sweeps reveal a supplementary but very small step at 250 mV. Nevertheless, the existence of two steps is in this case, homogeneous with that has been observed for the lower values of selenium.

The stoichiometry determined by the microanalysis shows a homogeneous intercalation with a content equal to 2.14 in agreement with the X-ray diffraction pattern.

A partial substitution with selenium in the Mo_6S_8 unit logically modifies the voltamperograms. They give evidence for a progressive change from four steps observed for Mo_6S_8 to the rather unique one in the case of the Mo_6S_8 binary. The maximum uptake of guest ions (number of copper atoms to enter the structure) is strongly correlated to the sulfur content (x) of the cathode material. For instance, the maximum of copper content decreases from 4 to 2.14 as x decreases from 8 to 0, except for $x = 4$ where an insertion rate of 1.67 is observed. This latter result is difficult to explain rationally. Nevertheless, the shape of the $i = f(E)$ curves depictes this trend, namely, the increase of insertion rate follows the increase of insertion signal number.

The lower potentials for the first intercalation systems observed in richer selenium compounds might basically be due either to a higher kinetic hindrance of the copper ions transport in the solid phase or to a lower thermodynamic stability of selenide phases compared to the sulfide compounds. Since the peak gaps for a step (defined as the difference between anodic and cathodic peak potentials) remain approximatively constant whatever the selenium content, the intercalation phenomenon does not seem to be directly related to the cation diffusion in the solid. On this basis, one would retain the second possibility. Among the chalcogenides compounds, a higher free energy of reaction has always been observed for the sulfides than for the selenides. Our results confirm these observations.

The results of the structural investigations for the different intercalated phases reveal changes in lattice parameters (an increase of a_H concomitant with a decrease of c_H). The intercalation logically induces an increase of cell volume. Another point to note is the good correlation between the copper content determined by X-ray and microanalysis data.

V.2. β-$Mo_6Se_{8-x}S_x$

The β-$Mo_6Se_{8-x}S_x$ pseudo-ternaries are obtained by heating the α-equivalent ones. Indeed, from 470°C, a partial decomposition of α-compounds in $Mo_6Se_{2-z}S_z$ and molybdenum, simultaneously followed by a Mo self-intercalation

leads to the new sulfoselenide series. Note that $MoSe_{2-z}S_z$ phases in the final products are always, of course, observed (1, 9, 10). Before undertaking a comparative study on the copper intercalation, we had to ensure that the electrochemical response was not disturbed by the presence of $MoSe_{2-z}S_z$. A simple way to test this eventuality is to cycle a $MoSe_{2-z}S_z$ cathode in a copper solution. We observed the absence of detectable signal whatever the tested compounds (MoS_2, $MoSe_1S_1$, $MoSe_2$). In our conditions, the electrochemical insertion of copper into $MoSe_{2-z}S_z$ can be completely ruled out. X-ray patterns substantiate this suggestion.

Electrochemical data from electrodes based on β-$Mo_6Se_{8-x}S_x$ are plotted in Figs. 4a–e.

β-Mo_6S_8, $x = 8$. A striking feature is the different behavior of this material with respect copper intercalation. First, we had to decrease the potential sweep rate in order to bring evidence for a possible insertion. The electrode response with a potential sweep rate similar to the ones previously used is not very representative of a phenomenon because of less well-defined peaks and of the signal intensities that are very small. However, the signals show a reversible intercalation process. Another interesting point is the fact that the curve does not surimpose on the first one obtained with α-Mo_6S_8. The intercalation systems are displaced to lower potentials and indicate lower free energy reactions. These observations led us to conclude the difficulty even the inability of this β-Mo_6S_8 material to intercalate copper not only on surface sites but also inside the crystallites. This is clearly demonstrated by the X-ray diffraction. There are very slight changes in lattice parameters (Table 2). The result of the microanalysis indicates a low content of 0.28 copper by Mo_6S_8 unit while the content of extra Mo does not vary. This behavior may simply result from structural factors as we will discuss below.

β-$Mo_6Se_2S_6$, $x = 6$. In contrast with the β-Mo_6S_8 binary, the cyclic voltammetry investigations (Fig. 4b) on the Cu/β-$Mo_6Se_2S_6$ system demonstrate a higher ionic mobility of Cu ions in the $Mo_6Se_2S_6$ framework. The curve exhibits several signals, though they are poorly differentiated. The appearance of successive steps is probably due to the existence of different types available lattice sites. Moreover, the reduction process begins at 300 mV. The electrochemical formation of β-$Cu_yMo_6Se_2S_6$ is easier than that of β-$Cu_yMo_6S_8$. The value of copper content (1.68) and

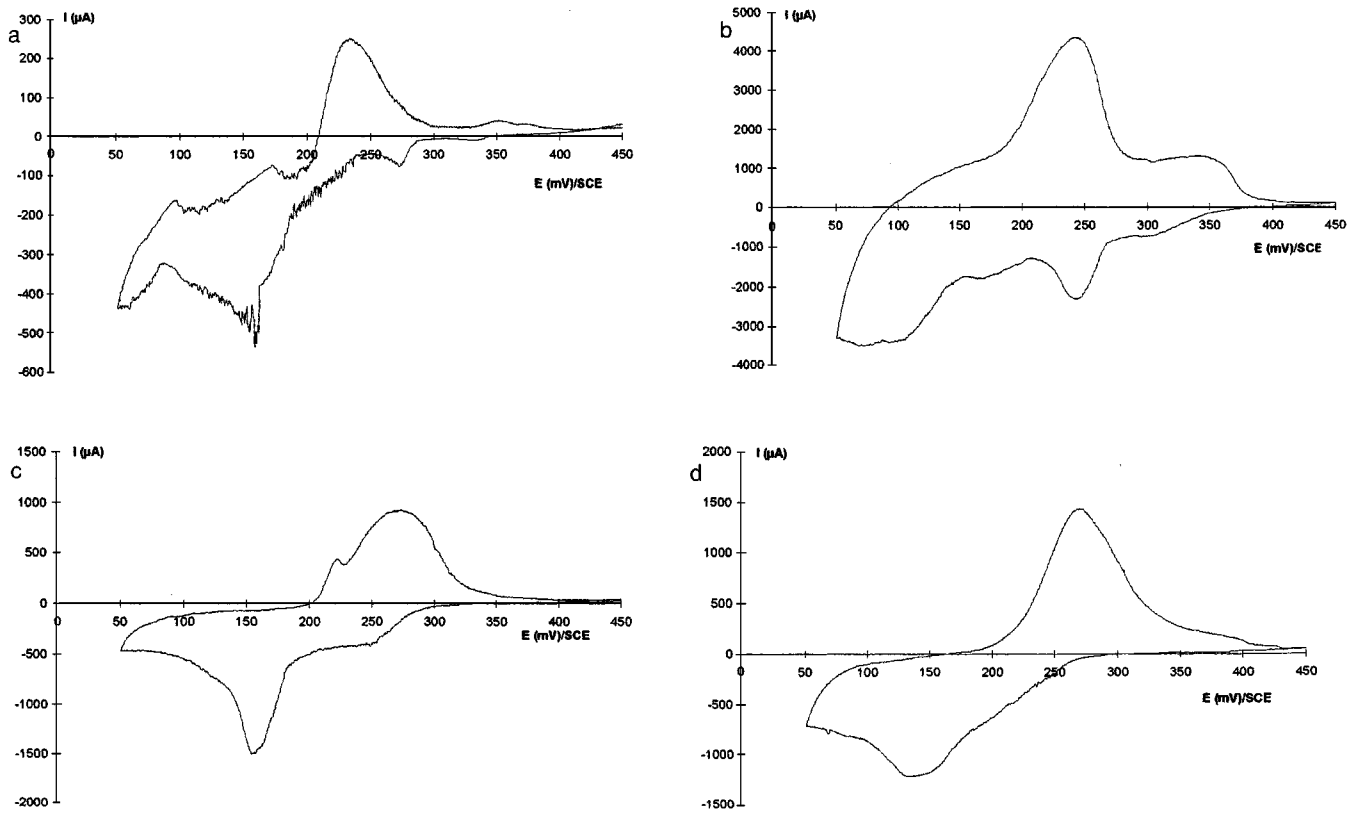

FIG. 4. Voltamperograms for β-$Mo_6Se_{8-x}S_x$ compounds in 1 M $CuSO_4$ medium, supporting disk area, $s = 6.2\ mm^2$, temperature $T = 60°C$, scan rate $v = 5\ mV\ min^{-1}$ (for a) and $v = 10\ mV\ min^{-1}$ (for b–e): (a) $x = 8$, (b) $x = 6$, (c) $x = 4$, (d) $x = 2$, (e) $x = 1$.

TABLE 2
Hexagonal Lattice Parameters, Unit Cell Volumes, Analytical Data of β-$Mo_6Se_{8-x}S_x$ Pseudo-Ternaries and β-$Cu_yMo_6Se_{8-x}S_x$ Compounds Prepared by Cathodic Reduction in Copper Aqueous Electrolyte

Phase	Parameters of initial binary			Parameters of intercalated compound			Cu content determined by microprobe analysis	Observations and Cu conent estimation from literature data
	a_h (Å)	c_h (Å)	V_h (Å^3)	a_h (Å)	c_h (Å)	V_h (Å^3)		
β-Mo_6S_8	9.09	11.27	804	9.08	11.29	807	0.28	≈ 0
β-$Mo_6Se_2S_6$	9.39	10.68	816	9.56	10.39	821	1.68	Interaction $<$ Cu content in α-equivalent component
β-$Mo_6Se_4S_4$	9.47	10.77	836	9.77	10.48	866	1.67	< 2 (24)
β-$Mo_6Se_6S_2$	9.56	10.88	861	9.84	10.62	889	1.52	2.6 (12)

structural data (Table 2) confirm the above trend and agree quite well with the electrochemical data.

β-$Mo_6Se_4S_4$, $x = 4$. Figure 4c shows the voltamperograms of β-$Mo_6Se_4S_4$. The curve is less complex in comparison with the precedent one. The insertion arises in two successive steps. The second signal (150 mV) is the most important. In the course of the oxidation process, one global oxidation peak with a shoulder is distinguished. The position and the importance of signals are homogeneous with those observed for the α-equivalent binary consistent with a similar behavior for both phases. This is confirmed by either the crystallographic (Table 2) or analytical data (equivalent cationic content).

β-$Mo_6Se_6S_2$, $x = 2$. The shape of the $i = f(E)$ curve (Fig. 4d) is closely similar to that for Cu/α-$Mo_6Se_6S_2$ system (two insertion steps and one wide anodic signal). Microanalysis confirms the formation of an intercalated compound but with a copper content slightly inferior to that of α-$Mo_6Se_6S_2$. A smaller variation of the lattice parameters (Table 2) is observed from $a_H = 9.84$ Å and $c_H = 10.62$ Å ($V_H = 889$ Å^3) to $a_H = 9.94$ Å and $c_H = 10.60$ Å ($V_H = 907$ Å^3) for the β- and α-$Cu_yMo_6Se_6S_2$ compounds, respectively.

The β-sulfoselenide compounds show intercalation process resulting in compounds of formula β-$Cu_yMo_6Se_{8-x}S_x$ (or better $(Cu_yMo_z)Mo_6Se_{8-x}S_x$). A simple displacement between copper and molybdenum (2) is to be ruled out because the initial molybdenum (2) content remains constant after copper intercalation.

The Mo_6X_8 phases present two types of sites available for intercalation, a large pseudo-cubic cavity (site 1) compressed along the 3-fold axis and six other small and very distorted cavities (site 2) forming a kind of octahedron around the 3-fold axis. If both sites are empty in α-binaries, they are partially occupied in β-$Mo_6Se_{8-x}S_x$ series. The cavity 1 (inner site) is filled by Mo atom in β-Mo_6S_8 leading to $Mo_{1.18}Mo_6S_8$. In contrast, the ternary molybdenum atom sits in the outer site 2 for β-$Mo_6Se_{8-x}S_x$ ($x \neq 8$). These phases present another difference with the previous binary, the guest molybdenum content is much lower ($Mo_{max} = 0.41$ for $x = 6$).

As copper intercalation into β-Mo_6S_8 proceeds, the copper ions could first occupy the small tetrahedral sites in the cavities (2), but their migration into the channels will be blocked by Mo atoms (amount larger than one) sitting on the cavity (1). Furthermore, the existence of a large energy barrier between outer sites of neighboring clusters according to the model proposed by Dudley enhances this impossibility of migration. Besides, the size of copper ion is certainly not large enough to liberate the inner sites occupied by Mo. The intercalation of copper atoms into β-Mo_6S_8 induces no changes in the unit cell volume. This implies that the $Mo_{1.8}Mo_6S_8$ matrix does not expand and the displacement of $(Mo)_2^{2+}$ does not take place by an overintercalation of copper contrary to the case with lithium alluded to above. The electrochemical data (absence of quantitative signals, lower potentials) are consistent with these observations. Our analytical data which show that the copper content in β-Mo_6S_8 is close to zero (0.28) and the molybdenum one is constant strongly support the above assumptions.

For the β-$Mo_6Se_{8-x}S_x$ ($x \neq 8$), the situation is totally different. Crystallographic studies on $Cu_yMo_6Se_{8-x}S_x$ ($y = 1.8$) compounds obtained by ceramic way have shown that copper atoms first occupy the inner site (cavity (1)). As copper is electrochemically introduced into the α-host lattice, it can sit on the available cavity (cavity (1)). In continuation of the reduction process, it appears that the guest cation would have to occupy tetrahedral sites (cavity (2)) which are partially filled with Mo atoms. It is conceivable that the presence of atom in this second cavity slows down but does not prevent the copper transport. On this basis, one would expect an electrochemical intercalation into β-$Mo_6Se_{8-x}S_x$ to be less easy than into α-phases leading to a shift to the lower free energy potentials. This conclusion is verified through voltamperograms. Another remarkable finding arises from the copper content. Since sites 2 were equally occupied in pseudobinaries, one would expect the

ion content intercalated into these phases, on the one hand, to be independent of selenium substitution and, on the other hand, to be smaller than that observed in α-homologue phases. This is clearly demonstrated by the analytical data, within their accuracy. The maximum uptake of guest ions in these materials does not vary with the selenium content (1.52 to 1.68, inferior, in all cases, to the α-insertion rate).

V.3. HT-$Mo_6Se_{8-x}S_x$ from Direct Synthesis

We now briefly present the results of similar studies on Cu/high temperature HT-$Mo_6Se_{8-x}S_x$ systems. Only richer selenium phases ($x \leq 5$) can be synthesized directly. The high temperature phases present structural characteristics similar to those of β-homologue $Mo_6Se_{8-x}S_x$. The cell parameters are very close together. On this basis, one might expect molybdenum atoms to be incorporated into the lattice of high temperature binaries. In a recent study, S. Belin *et al.* have reported the structure of these latter phases (11). They have shown that Mo atoms are present in the same cavity in an equivalent proportion. Both findings suggest that the high temperature host materials behave as the β-phases with respect to copper intercalation.

The electrochemical curves are shown all together in Figs. 5a, 5b, and 5c for $Cu_yMo_6Se_{8-x}S_x$ where $x = 0$, 2, and 4.

A common feature is the shape of $i = f(E)$ which is quite similar to that exhibited by β-$Mo_6Se_{8-x}S_x$ electrodes (two less well-defined intercalation steps and one wide oxidation signal). Their position in potential scale shifts again but smoothly. The observed intensities would represent a complete transformation of initial binary. The X-ray patterns confirm the existence of intercalated compounds (Table 3). The lattice parameters, particularly the unit cell volumes, led us to conclude that the uptake of copper atoms into the ceramic phases is slightly lower. The microprobe analysis is in good agreement with this prediction.

Another point arises from the tiny difference in signals definition for α- and HT-Mo_6X_8 curves. This result may be explained in terms of granulometry. We have shown that the grain size parameter of samples can influence the shape of voltamperograms. The α-samples result from a chemical oxidation (by dilute hydrochloric acid) of ternary phases. This deintercalation causes some damage to the crystallites. Their size is decreasing. This fact is favorable to an enhancement of the diffusional phenomenon taking place inside the crystal.

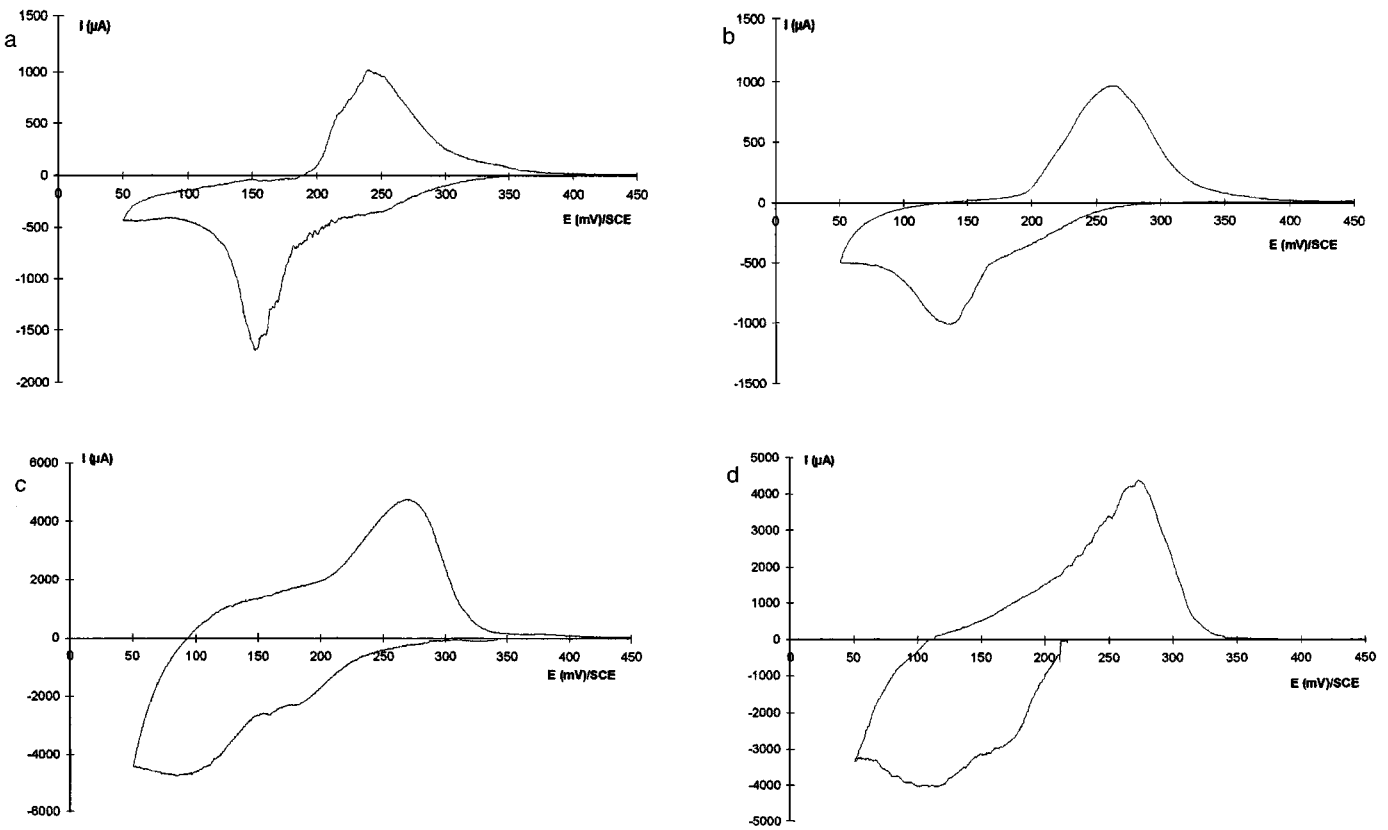

FIG. 5. Voltamperograms for high-temperature HT-$Mo_6Se_{8-x}S_x$ compounds in I M $CuSO_4$ medium, supporting disk area, $s = 6.2\,mm^2$, temperature $T = 60°C$, scan rate $v = 10\,mV\,min^{-1}$: (a) $x = 0$, (b) $x = 1$, (c) $x = 2$, (d) $x = 4$.

TABLE 3
Hexagonal Lattice Parameters, Unit Cell Volumes, Analytical Data of High Temperture HT-$Mo_6Se_{8-x}S_x$ Pseudo-Ternaries and HT-$Cu_yMo_6Se_{8-x}S_x$ Compounds Prepared by Cathodic Reduction in Copper Aqueous Electrolyte

Phase	Parameters of initial binary			Parameters of intercalated compound			Cu content determined by microprobe analysis	Observations and Cu conent estimation from literature data
	a_h (Å)	c_h (Å)	V_h (Å^3)	a_h (Å)	c_h (Å)	V_h (Å^3)		
HT-$Mo_6Se_4S_4$	9.53	10.67	838	9.75	10.45	860	1.47	< 2 (24)
HT-$Mo_6Se_6S_2$	9.57	10.87	862	9.83	10.61	888	1.58	< 2.6 (23)
HT-$Mo_6Se_7S_1$	9.58	10.99	874	9.88	10.70	905	1.42	Intercalation $<$ Cu content in α-equivalent compound

The chemistry of the intercalation into the Chevrel phase Mo_6X_8, for a fixed cation, depends upon the nature, the size, and the occupancy of the cavities as well as the electronic structural factors. The following paragraph will adress the outlines of the electrochemical behavior of the different binaries series with respect to copper insertion. Figure 6 shows the variation of the integral copper insertion rate as function of the sulfur content and the synthesis type of pseudobinaries. This figure provides evidence that the more α-rich sulfur phases have better intercalation capabilities than the richer selenium binaries. Such results may indicate the predominance of electronic factors since both available sites are empty. This point is clearly confirmed by the electrochemical curves. The number of intercalation steps increases and the position of signals shifts smoothly from lower to higher energy reaction with increasing sulfur content in the unit $Mo_6Se_{8-x}S_x$. The evolution of electrochemical reactivity of α-pseudobinaries is homogeneous with the variation of S/Se ratio.

Another striking fact is that the maximum ternary element content in materials not only correlates strongly to the presence of extra molybdenum atoms but also to the nature of occupied cavities. The β-Mo_6S_8 is a perfect illustration. Moreover, the insertion rate of β- and direct synthesis binaries are likely to be similar in agreement with the structural considerations (occupancy of cavity (2) by molybdenum atoms). The present work has revealed that the voltamperograms and their amplitude are also affected by these extra atoms in the channels and can be used to deduce structural informations. For instance, since the α- and HT-Mo_6Se_8 compounds have the same structure, one would expect the same electrochemical characteristics. Our study has revealed differences between these two binaries in their general shape of $i = f(E)$ curves and their intercalated cation rate. This anomaly can be ascribed either to an effect of granulometry like alluded to above or to the existence of very low extra molybdenum content into channels for the thermal phase not easily detectable.

This work has shown that the study of electrochemical reactivity of host lattices, through the examination of the voltamperograms, accounts for the structural states of different binaries forms and provides supplementary informations about the solid material which support even confirm the analytical and crystallographic data.

We have also found that molybdenum can never be removed from the β- and thermal binaries either by an electrochemical oxidation or by an electrochemical overintercalation displacement at room temperature. Since such temperatures are obviously uncompatible with a relatively high mobility of molydenum, the use of nonaqueous electrolytes that allow higher temperatures should improve the diffusional phenomenon.

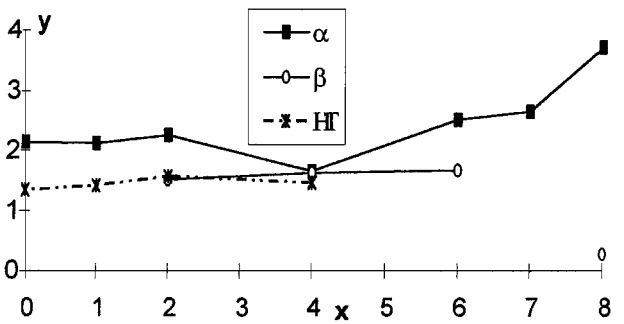

FIG. 6. Variation of copper content in α-, β-, and HT-$Mo_6Se_{8-x}S_x$ binary and pseudo-ternary compounds.

VI. CHEMICAL BEHAVIOR OF β-Mo_6S_8

VI.1. Chemical Deinsertion

The most used process to deintercalate cations from ternary Chevrel phases is the hydrochloric acid leaching. Of course, we first attempt this process on β-Mo_6X_8 and HT-Mo_6X_8. The X-ray diffraction patterns recorded on the products treated with this method show no change, and the "washing solutions" analyzed by absorption spectroscopy do not contain any molybdenum element.

So, we were interested in the method used by Potel *et al.* to deinsert indium from $InMo_6S_8$ (3). The method is based on the use of HCl gas flow passing on powdered compounds

heated at 300°C. At this temperature, $InCl_3$ is very volatile, so this reaction is very interesting to produce pure α-Mo_6S_8. In the same way we studied β-Mo_6S_8 but at about 600°C during 6 h. Quickly a release of molybdenum chloride is shown. The compound is then cooled under HCl gas to prevent the β-Mo_6S_8 from re-forming. A loss of weight with a Mo/Mo_6S_8 ratio of $\sim$1.08 can be detected on the compound after such a treatment. The X-ray diffraction pattern shows the obtained compound to be α-Mo_6S_8.

Elsewhere we have reported that this method was also efficient on the whole β- and HT-series. So, to remove Mo(2) guest atoms from the host we just need to increase the temperature of the method because molybdenum chloride is less volatile than InCl3, and moreover these Mo(2) atoms are bonded with either both to form quadruple bond (it is the β-Mo_6S_8 particular case) or with Mo(1) atoms to form kind of Mo_7 clusters (case of β-$Mo_6Se_{8-x}S_x$ ($x \neq 8$) and HT-$Mo_6Se_{8-x}S_x$ series) (10,11).

In $TRMo_6X_8$ (TR = rare earth element), $PbMo_6X_8$, and $SnMo_6X_8$ (X = Se or S), we recently showed that the cation can be removed with this last method at the same temperature. In general, the deintercalation activation energy depends on the inserted metal ion (unfavorable steric effects) and also on the bonding strengths acting on the metal ion. In the case of Mo(2) guest atoms, the latter predominates, while for Pb, Sn, or TR elements it is the size of cation which matters.

VI.2. Cationic Exchange

We have studied the overinsertion of small cations in β-Mo_6S_8 via ceramic routes at low enough temperature. The electrochemical study has shown that it is very difficult to insert copper cation in this compound. It seems that the highest copper amount should be 0.28 Cu/Mo_6S_8 unit. We have already reported that in β-Mo_6S_8, VEC is close to $22e/Mo_6$ exactly as for $PbMo_6S_8$. It was established that compounds with such a VEC should be very stable. Previous studies (13) have shown that overintercalation in $PbMo_6S_8$ was very low; so, for β-Mo_6S_8 a similar behavior could be expected. Then we attempt to exchange Mo(2) atoms for small cations as Cu or Ni, because it was reported in ternary Chevrel phases that small cations can expel bigger ones (for instance copper can be exchanged for lead). In the first part of this paper, we have seen that no Mo(2) atoms could be remove electrochemically from β-Mo_6X_8 and HT-Mo_6X_8 series because the method uses an aqueous electrolyte and therefore the reaction temperature is limited at ambient conditions. However, the electrochemical route is very efficient for overinsertion in these materials.

So we have carried out some experiments with copper element on β-Mo6S8 samples. Metallic copper powders in ratios of 0.5, 1, 2, or 3 copper atoms per Mo_6S_8 unit were added and closely mixed with β-Mo_6S_8. The mixture was slowly raised to 400°C for several days with intermediate rehomogenization. Most of time to complete the reaction we need to increase the temperature until 600°C. When the reaction is finished, the X-ray diffraction pattern always exhibits a mixture of $Cu_yMo_6S_8$ compounds with Mo element and MoS_2 binary (the latter comes from the initial β-Mo_6S_8 formation).

The cationic exchange reaction was only undertaken on β-Mo_6S_8 because the other β- or HT-$Mo_6Se_{8-x}S_x$ compounds do not contain enough Mo(2) atoms to detect Mo element by X-ray diffraction pattern if it is removed. β-Mo_6S_8 was the best example to simply carry out this study.

We also tried nickel cations. The result is still the same, Cu or Ni substitute for Mo(2) atoms in the cavity (1) of the channels.

Incomplete reactions at lower temperatures show that small amounts of Cu (or Ni) can be overinserted in β-Mo_6S_8. Effectively, we observe at the beginning of the reaction a mixture of two Chevrel phases: for instance, the reaction Cu + β-Mo_6S_8 at 400°C for 2 days gives one Chevrel phase with unit cell parameters very close to ones of β-Mo_6S_8 ($(Cu_{\sim 0.2}Mo)Mo_6S_8$: $a_H = 9.10$ Å, $c_H = 11.34$–11.35 Å, $V_H = 813$–815 Å^3) plus a second $Cu_yMo_6S_8$ phase ($y \sim 2.6$–2.7: $a_H = 9.66$ Å, $c_H = 10.213$ Å, $V_H = 825$ Å^3) with equivalent amounts. The longer the reaction and/or the higher the temperature, the more $Cu_yMo_6S_8$ amount increases with y decreasing to the detriment of the $\sim\beta$-Mo_6S_8 and Mo impurities appear. At 600°C, 48 h, the close β-phase disappears completely and we then observe only one $Cu_yMo_6S_8$ phase ($y \sim 2$: $a_H = 9.59$ Å, $c_H = 10.235$ Å, $V_H = 815$ Å^3) with much more Mo and, of course, MoS_2.

We observe exactly the same phenomena with the 2 Cu, and more with the same close β-phase and $Cu_yMo_6S_8$ ($y \sim 2.8$–2.0). From these observations, we can conclude that a very few copper atoms can be overintercalated in the network but the overinsertion of copper atoms involves the removal of molybdenum atoms. These results confirm the electrochemical investigations previously obtained on this compound.

VII. CONCLUSION

We reported the electrochemical insertion of copper atoms into three series of $Mo_6Se_{8-x}S_x$ phases. We showed that α-, β-, and HT-forms can accommodate copper. The copper content decreases from α- binaries to β- and HT-ones. A striking difference has been observed in the behavior of β-Mo_6S_8. This phase practically does not intercalate with copper. We showed that such a behavior might be explained in terms of available vacant sites. In general, structural changes and analytical data correlate perfectly with the electrochemical curves. Finally, the voltamperograms can be used as "chimie douce" potential photographs for any

material. The electrochemical curves can evidence the reactivity and reflect the structural state of host lattices.

Chemical copper insertions in β-Mo_6S_8 show cationic exchange reactions if the reaction is complete otherwise a slight overinsertion of copper cations in the host. Chemical methods, such as HCl gas flow, indicate that Mo(2) guest atoms can be deintercalated from the β-Mo_6X_8 and HT-Mo_6X_8 series. All these studies exhibit the high enough mobility of the Mo(2) guest atoms in the Chevrel phases.

REFERENCES

1. R. Chevrel and M. Sergent, *in* "Topics in Current Physics" (Ø. Fischer and M. B. Maple, Eds.), Vol. 32, p. 25. Springer Verlag, Berlin, 1982.
2. Ø. Fischer, *Appl. Phys.* **16,** 1 (1978).
3. R. Chevrel, M. Sergent, and J. Prigent, *Mater. Res. Bull.* **9,** 1487 (1974). M. Potel, P. Gougeon, R. Chevrel, and M. Sergent, *Rev. Chim. Minéral.* **21,** 509 (1984).
4. R. Schöllhorn, M. Kümpers, and J. O. Besenhard, *Mater Res. Bull.* **12,** 781 (1977). R. Schöllhorn, *Angew. Chem.* **92,** 1015 (1980).
5. J. M. Tarascon, J. V. Waszczak, G. W. Hull, F. J. Di Salvo, and L. D. Blitzer, *Solid State Commun.* **47,** 973 (1983). J. M. Tarascon, F. J. Di Salvo, D. W. Murphy, G. W. Hull, E. A. Rietman, and J. V. Waczczak, *J. Solid State Chem.* **54,** 204 (1984). J. M. Tarascon, F. J. Di Salvo, D. W. Murphy, G. W. Hull, and J. V. Waszczak, *Phys. Rev. B* **29,** 172, (1984). J. M. Tarascon, F. J. Di Salvo, J. V. Waszczak, and G. W. Hull, *Phys. Rev. B* **31,** 1012 (1985). J. M. Tarascon, J. V. Waszczak, F. J. Di Salvo, and D. C. Johnson, *Solid State Commun.* **53,** 849, (1985).
6. G. J Dudley and B. C. H. Steele, *J. Solid State Chem.* **32,** 233 (1980).
7. C. Boulanger and J. M. Lecuire, *Electrochim. Acta* **32**(2), 345 (1987). C. Boulanger, and J. M. Lecuire, *Solid State Ionics*, **25,** 45 (1987).
8. Umarji, G. V. Subba Rao, M. P. Janawadkar, and T. S. Radhakrishnan, *J. Phys. Chem.* **41,** 421 (1980).
9. S. Belin, R. Chevrel, and M. Sergent, *Mater. Res. Bull.* **33**(1), 43 (1998).
10. S. Belin, L. Burel, M. Sergent, and R. Chevrel, *Mater. Res. Bull.*, to be published.
11. S. Belin, R. Chevrel, and M. Sergent, *J. Solid State Chem.* accepted for publication.
12. K. Yvon, *in* "Current Topics in Materials Science" (E. Kaldis, Ed.), Vol. 3, p. 53. North Holland, Amsterdam, 1979.
13. M. Sergent, R. Chevrel, C. Rossel, and Ø. Fischer, *J. Less-Common Met.* **58,** 179 (1978). R. Chevrel, C. Rossel, and M. Sergent, *J. Less-Common Met.* **72,** 31 (1980). F. Y. Fradin, and J. W. Downey, *Mater. Res. Bull.* **14,** 1525 (1979).
14. R. Schöllhorn, M. Kümpers, A. Lerf, E. Umlauf, and W. Schmidt, *Mater. Res. Bull.* **14,** 1039 (1979).
15. M. Tovar, L. Delong, D. G. Johnson, and M. B. Maple, *Solid State Comm.* **30,** 551 (1979).
16. G. J. Dudley, K. Y. Cheung, and B. C. H. Steele, *J. Solid State Chem.* **32,** 259 (1980).
17. P. J. Mulhern and R. R. Haering, *Can. J. Phys.* **62,** 527 (1984).
18. T. Uchida, K. Watanabe, M. Wakihara, and M. Taniguchi, *Chem. Lett.* 1095 (1985). M. Wakihara, T. Uchida, T. Morishita, H. Wakamatsu, and M. Taniguchi, *J. Power Sources* **20,** 199 (1987). M. Wakihara, T. Uchida, K. Suzuki, and M. Taniguchi, *Electrochim. Acta* **34,** 867 (1989). T. Uchida, Y. Tanjo, M. Wakihara, and M. Taniguchi, *J. Electrochem. Soc.* **137,** 7 (1990). S. Yamaguchi, T. Uchida, and M. Wakihara, *J. Electrochem. Soc.* **138,** 687 (1991).
19. J. M. Tarascon, T. P. Orlando, and M. J. Neal, *J. Electrochem. Soc.* **135,** 804 (1988).
20. W. R. Mc Kinnon and J. R. Dahn, *Solid State Commun.* **52,** 245 (1984).
21. C. Boulanger and J. M. Lecuire, *Electrochim. Acta* **33**(11), 1577 (1988).
22. K. Yvon, A. Paoli, R. Flükiger, and R. Chevrel, *Acta Crystallogr. B* **33,** 3066 (1977).
23. L. S. Selwyn, W. R. Mc Kinnon, J. R. Dahn, and Y. Le Page, *Phys. Rev. B* **33,** 6405 (1986).
24. L. S. Selwyn, W.R. Mc Kinnon, and Y. Le Page, *Phys. Rev. B* **42,** 10427 (1990).